

DIRECT OBSERVATIONS OF SUBMICROPULSE ELECTRON-BEAM EFFECTS FROM SHORT-RANGE WAKEFIELDS IN TESLA-TYPE SUPERCONDUCTING RF CAVITIES*

A.H. Lumpkin^{#1}, R. Thurman-Keup¹, D. Edstrom Jr.¹, P. Prieto¹, J. Ruan¹,
B. Jacobson², A. Edelen², J. Diaz-Cruz², F. Zhou²

¹Fermi National Accelerator Laboratory, Batavia, IL 60510 USA

²SLAC National Accelerator Laboratory, Menlo Park, CA 94025 USA

Abstract

Experiments were performed at The Fermilab Accelerator Science and Technology (FAST) facility to elucidate the effects of short-range wakefields (SRWs) in TESLA-type rf cavities. FAST has a unique configuration of a photocathode rf gun beam injecting two TESLA-type single cavities (CC1 and CC2) in series prior to the cryomodule. To investigate short-range wakefield effects, we have steered the beam to minimize the signals in the higher-order mode (HOM) detectors of CC1 and CC2 for a baseline, and then used a vertical corrector between the two cavities to steer the beam off axis at an angle into CC2. A Hamamatsu synchroscan streak camera viewing a downstream OTR screen provided an image of y-t effects within the micropulses with ~10-micron spatial resolution and 2-ps temporal resolution. At 500 pC/b, 50 b, and 4 mrad off-axis steering into CC2, we observed an ~ 100-micron head-tail centroid shift in the streak camera image y(t)-profiles. This centroid shift value is 5 times larger than the observed HOM-driven centroid oscillation within the macropulse, and it is consistent with a calculated short-range wakefield effect using ASTRA simulations.

INTRODUCTION

The preservation of the low emittance of electron beams during transport through the accelerating structures of large facilities is an ongoing challenge. In the cases of the TESLA-type superconducting rf cavities currently used in the European X-ray Free-electron Laser (FEL) [1] and the currently-under-construction Linac Coherent Light Source upgrade (LCLS-II XFEL) [2], off-axis beam transport may result in emittance dilution due to transverse long-range (LRW) and short-range wakefields (SRW) [3-5]. To investigate such effects, experiments were performed at the Fermilab Accelerator Science and Technology (FAST) facility with its unique two-cavity configuration after the photocathode rf gun [6]. We used optical transition radiation (OTR) imaging with a UV-visible synchroscan streak camera to display sub-micropulse y-t effects in the 41-MeV beam.

We report effects on beam transverse position centroids and sizes correlated with off-axis beam steering in TESLA-type cavities. We used a 3-MHz micropulse repetition rate

and targeted diagnostics for these tests. Our initial data from an OTR imaging source indicated our streak camera can provide ~10-micron spatial resolution with 1-2 ps (σ) temporal resolution depending on the bandpass filter employed. Since the observed bunch lengths were 10-20 ps (σ), we had sufficient resolution for up to 20 time slices in the 4σ profile. In this sense we also obtained slice-emittance information (with β -function information). We used the higher-order mode (HOM) detectors and rf BPMs to establish first the desired off-axis steering and then evaluated the short-range wakefield effects on the beam dynamics.

EXPERIMENTAL ASPECTS

The IOTA Electron Injector Linac

The Integrable Optics Test Accelerator (IOTA) electron injector at the FAST facility (Fig. 1) begins with an L-band rf photoinjector gun built around a Cs₂Te photocathode (PC). When the UV component of the drive laser, described elsewhere [7] is incident on the PC, the resulting electron bunch train with 3-MHz micropulse repetition rate exits the gun at <5 MeV. Following a short transport section with a pair of trim dipole magnet packages (H/V100 and H/V101), the beam passes through two superconducting rf (SCRF) capture cavities denoted CC1 and CC2, and then a transport section to the low-energy electron spectrometer, D122. Diagnostics used in these studies include the rf BPMs, the imaging screens at X107, X108, X121, and X124, and HOM couplers at the upstream and downstream ends of each SCRF cavity. The HOM signals were processed by the HOM detector circuits with the Schottky diode output provided online through ACNET, the Fermilab accelerator controls network [4]. The HOM detectors' bandpass filters were optimized for two dipole passbands from 1.6 to 1.9 GHz, and the 1.3-GHz fundamental was reduced with a notch filter. The rf BPMs' electronics were configured for bunch-by-bunch capability with optimized system attenuation. At 2 nC per micropulse, the rms noise was found to be 25 μ m in the horizontal axis (x) and 15 μ m in the vertical axis (y) at B101 in the test with 4.5-MeV beam from the gun. However, for these studies on short-range transverse wakefields, we relied on a streak camera to provide the sub-micropulse spatial information.

The Streak Camera System

We utilized a C5680 Hamamatsu streak camera with an S20 PC operating with the M5675 synchroscan vertical

*This manuscript has been authored by Fermi Research Alliance, LLC under Contract No. DE-AC02-07CH11359 with the U.S. Department of Energy, Office of Science, Office of High Energy Physics.

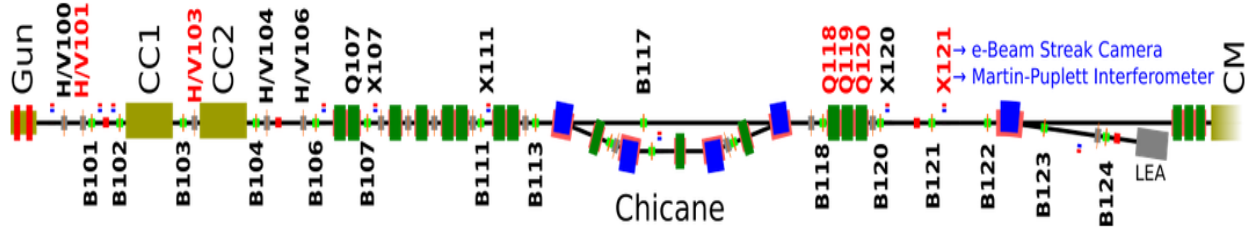


Figure 1: Schematic of the FAST beamline layout showing the PC rf gun, capture cavities (CCn), correctors (H/Vnnn), rf BPMs (Bnnn), chicane, OTR and YAG:Ce screens (Xnnn), the spectrometer dipole bend magnet (D122), and the beginning of the cryomodule (CM).

deflection unit that was phase locked to 81.25 MHz as shown in Fig. 2. In addition, we used a phase-locked-loop C6878 delay box that stabilizes the streak image positions to about 1 ps temporal jitter over 10s of minutes. These steps enabled the synchronous summing of 50-150 micropulses or bunches (b) generated at 3 MHz by the photoinjector or the offline summing of 10-100 images to improve statistics in the sum images. We applied the principle to optical transition radiation (OTR) generated from an Al-coated Si substrate at the X121 screen location (see Fig. 1) with subsequent transport to the beamline streak camera. Commissioning of the streak camera system was facilitated through a suite of controls centered around ACNET. This suite includes operational drivers to control and monitor the streak camera as well as Synoptic displays to facilitate interface with the driver. Images were captured from the streak camera using the readout camera, Prosilica 1.3-Mpixel cameras with 2/3" format, and were analyzed both online and with an offline MATLAB-based ImageTool processing program [8]. Bunch-length measurements using these techniques have been reported previously from the A0 Facility [9] and FAST first system streak camera commissioning at 20 MeV [10].

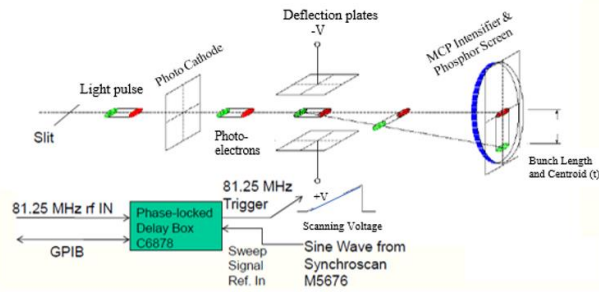


Figure 2: Schematic of the C5680 synchroscan streak camera with phase locking at 81.25 MHz.

EXPERIMENTAL RESULTS

Initial Streak Camera Data:

In order to investigate the short-range, wakefield-driven submicropulse effects, we used the HOM detector signals as a measure of how far off axis the beam was in the cavities. We minimized the HOMs in CC1 and CC2 as the

reference point, and then stepped the V103 corrector magnet current values. For the 24-MeV post-CC1 beam energy, a change of 1 A in corrector current corresponded to a 2-mrad angular steering change into CC2. The transport optics rotated the image 90° so we observed the vertical spatial information on the horizontal display axis in the streak image from X121. The changes in projected vertical beam profile size are shown in Fig. 3a. Beam size dilution is clearly seen at 650 μm compared to the 400-μm cases. In Fig. 3b, the head-tail kick directions follow the

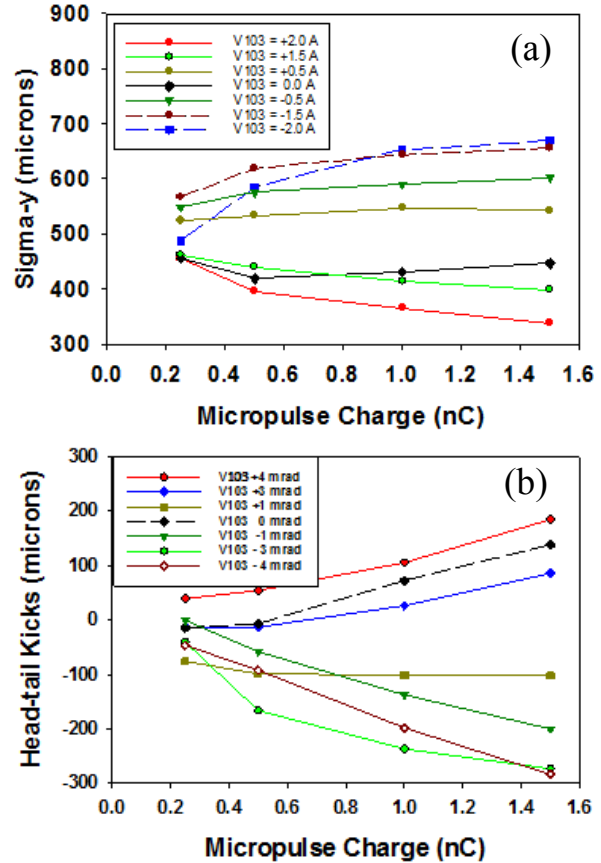


Figure 3: (a) Projected vertical beam profiles for X121 streak camera images versus charge at various V103 corrector values. (b) Observed head-tail centroid kicks for the same images as a function of charge and V103 corrector values. A 1-A corrector current change corresponds to a 2-mrad angular steering change into CC2.

corrector steering polarity as expected. These data exhibit the direction the beam is off axis while the HOMs with the electronics used indicate only the offset magnitude. These combined effects may be used in a future machine learning training application to mitigate emittance dilution effects.

Space-Charge-Driven Bunch Elongation effects

The streak images when projected to the time axis provide the electron bunch profile and length. With an initial laser pulse length of 4 ps, we observed the significant electron bunch elongation due to space-charge forces as seen in Fig. 4. In this case the laser spot size was ~ 0.45 mm by 0.56 mm so at 250 pC/b and above the space-charge forces dominated the distributions.

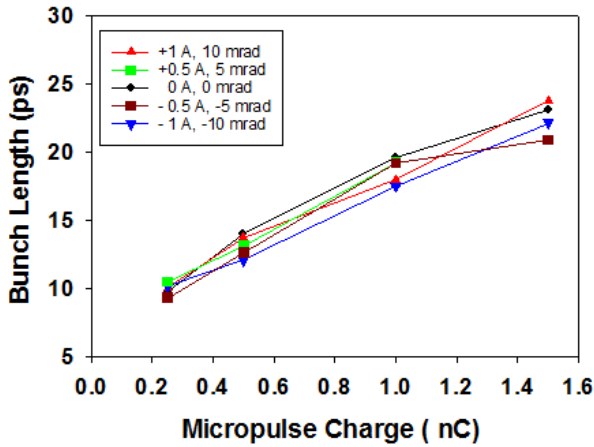


Figure 4: Streak camera bunch length versus charge results during the V101 corrector scan from -1.0- to +1.0-A values. At 4.5 MeV, a 1-A current change corresponds to a 10-mrad angular change into CC1. The transverse laser spot is ~ 0.5 mm in x and y in this case.

Bunch by Bunch rf BPM Data

We also evaluated the potential long-range wakefield or HOM effects on the beam centroid by using the rf BPM data. An example of the centroid motion *within* the 50-micropulse train of a macropulse is shown in Fig. 5 with both noise-reduction and bunch-by-bunch capabilities implemented. The 100-kHz oscillation seen in the B117 data is a difference frequency between HOM mode 14 in CC2 and a beam harmonic [4]. The field oscillations kicked different micropulses according to the amplitude at that point in time, resulting in the submacropulse effects. The quadrupole triplet Q118-120 was used to focus the beam smaller horizontally while leaving the vertical size at ~ 800 μm at the X121 YAG:Ce station. The beam centroid oscillation amplitude is much reduced to <20 μm at B121 downstream of this triplet, and thus the main competing mechanism identified does not account for the observed y-t effect in the streak image. Since the ASTRA simulation for the FAST setup indicated a 400- μm head-tail kick for 500 pC/b and a 5-mm offset at 41 MeV, we attribute the 100- μm head-tail effects for a 2-3 mm offset seen in Fig. 3 to such short-range wakefields [11].

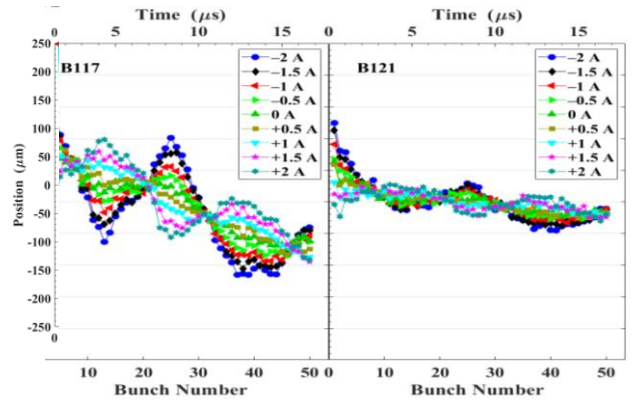


Figure 5: Examples of the variation of the beam vertical centroids bunch by bunch for 50 micropulses at B117 and B121 for V103 settings of ± 2 A from the reference. These were 100-shot averages to show the 100-kHz oscillation effects generated in CC2.

ASTRA Simulations of the Short-range Wakefield

The ASTRA simulations used the nominal FAST linac input deck with the laser bunch length of 4 ps sigma, a laser transverse spot size of 1.2 mm in x and y, an injection phase of 45° , a gun gradient of 45 MV/m, and the capture cavity gradients of 21 and 14 MV/m for CC1 and CC2, respectively. In particular, the program utilizes the 3D fields of the TESLA-type cavities to produce realistic simulations of the beam through the cavities for comparison to the observations. The simulations were for a single micropulse with 500 pC of charge transiting the two cavities with 0 mm and 5 mm offsets as shown in Fig. 6.

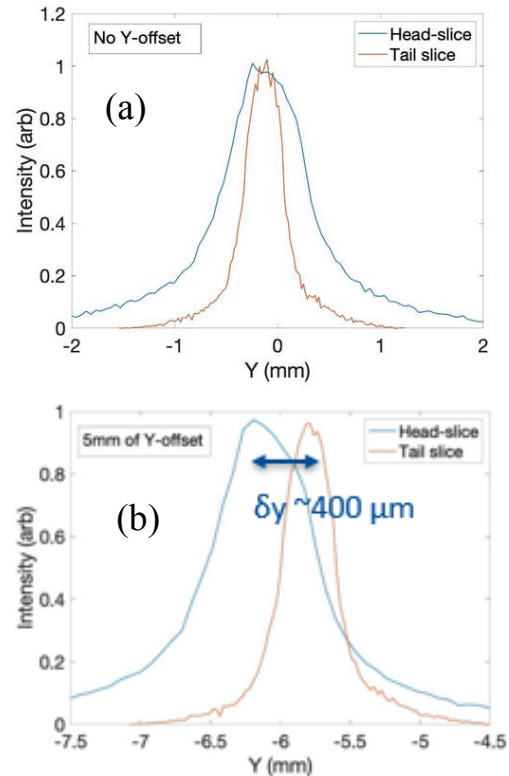


Figure 6: ASTRA simulation results of the head-tail kick for (a) no y offset and (b) 5-mm y offset through the cavities with a calculated ~ 400 - μm head-tail kick.

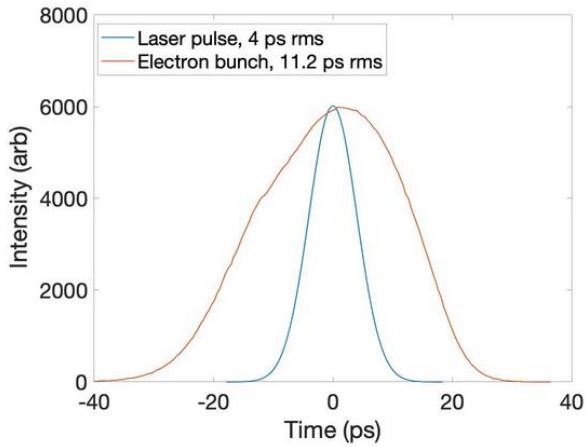


Figure 7: ASTRA simulation results for the electron-beam bunch length at 500 pC/b compared to the initial laser pulse length.

The time-sliced vertical distributions at the head and tail of the micropulse are shown. The simulation shows a tear-drop shape in y - t space (envison later time upward) as reported previously [5] and an approximately 400- μm head-tail kick for the 5-mm offset in Fig. 6b.

In Fig. 7 the elongation of the electron bunch is calculated as $\sigma_t = 11.2$ ps compared to the 4-ps laser pulse. This is attributed to space-charge forces acting before acceleration in CC1. The charge dependence of the bunch length from ASTRA is shown in Fig. 8 for the laser transverse spot size of 1.2 mm and the initial laser pulse of 4-ps duration. The electron beam rms bunch length varies from ~ 10 to 14 ps for 0.25 to 1.5 nC/b, respectively. There would be an expected increase in this effect for a smaller laser spot size of 0.5 mm as seen in the Fig. 4 data.

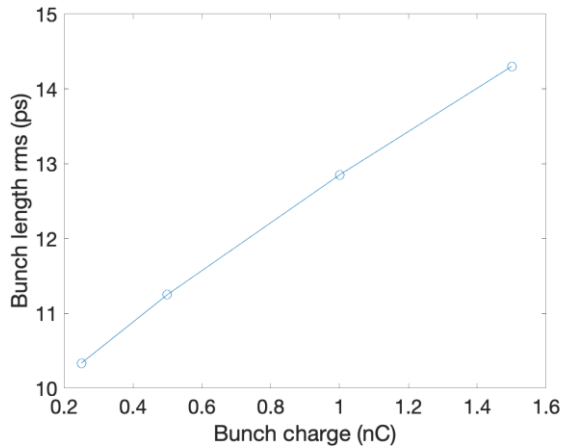


Figure 8: ASTRA simulation results for the charge dependence of the observed bunch length after CC2. The laser pulse length was 4 ps.

SUMMARY

In summary, observations of short-range wakefield effects on beam dynamics were made using the streak camera to obtain y - t images at the submicropulse time scale. The HOM detectors and rf BPMs were used to evaluate off-axis steering related to these tests, and the HOM-induced sub-macropulse centroid motion was shown to be much smaller than the observed effects. Moreover, the head-tail centroid kicks were consistent with short-range wakefield results from ASTRA for the TESLA-type superconducting rf cavity and attributed to that effect.

ACKNOWLEDGMENTS

The Fermilab authors acknowledge the support of C. Drennan, A. Valishev, D. Broemmelsiek, G. Stancari, and M. Lindgren, all in the Accelerator Division at Fermilab. The SLAC/NAL authors acknowledge the support of J. Schmerge (Superconducting Linac Division, SLAC).

REFERENCES

- [1] H. Weise, “Commissioning and First Lasing of the European XFEL”, Proc. of FEL17, MOC03, Santa Fe, NM, www.JACoW.org.
- [2] P. Emma, “Status of the LCLS-II FEL Project at SLAC”, Proc. of FEL17, MOD01, Santa Fe, NM, www.JACoW.org.
- [3] J. T. Seeman et al., “Transverse wakefield control and feedback in the SLC linac”, SLAC National Accelerator Laboratory Report No. SLAC-Pub-4182, 1987.
- [4] A.H. Lumpkin et al., “Submacropulse electron-beam dynamics correlated with higher-order modes in Tesla-type superconducting rf cavities, Phys. Rev. Accel. and Beams **21**, 064401 (2018).
- [5] A.H. Lumpkin, R.M. Thurman-Keup, D. Edstrom, J. Ruan, “Submicropulse electron-beam dynamics correlated with short-range wakefields in Tesla-type superconducting rf cavities”, Phys. Rev. Accel. and Beams **23**, 054401 (2020).
- [6] The ASTA User Facility Proposal, Fermilab-TM-2568, October 2013.
- [7] J. Ruan, M. Church, D. Edstrom, T. Johnson, and J. Santucci, Proc. of IPAC13, WEPME057, www.JACoW.org.
- [8] R. Thurman-Keup, FNAL, off-line MATLAB-based ImageTool (2011).
- [9] A.H. Lumpkin, J. Ruan, and R. Thurman-Keup, Nucl. Instr. and Meth. **A687**, 92-100 (2012).
- [10] A.H. Lumpkin, D. Edstrom, and J. Ruan, “Initial Demonstration of 9-MHz Framing Camera Rates”, Proc. of NAPAC16, TUPOA25, www.JACoW.org.
- [11] V. Lebedev (private communication, May 2016).